Antares Prototype 300-kJ, 250-kA Marx Generator

Final Report

University of California

LOS ALAMOS SCIENTIFIC LABORATORY
Post Office Box 1663 Los Alamos, New Mexico 87545

LA-8491

UC-21
Issued: January 1981

Antares Prototype 300-kJ, 250-kA Marx Generator

Final Report

Kenneth B. Riepe
L. L. Barrone
K. James Bickford
Glen H. Livermore

ANTARES PROTOTYPE 300-kJ, 250-kA MARX GENERATOR FINAL REPORT

by

Kenneth B. Riepe, L. L. Barrone,
K. James Bickford, and Glen H. Livermore

ABSTRACT

A high-energy, low-inductance, low prefire rate, low trigger jitter, high-voltage, pulsed-power supply was needed to drive the gas discharge in the Antares laser power amplifier. This report describes the design and testing of a Marx generator that meets these requirements, the development and testing of a high-capacity spark gap, and the selection of suitable capacitors and resistors.

I. INTRODUCTION

The power-amplifier design for the Antares 100-kJ CO_2 laser system at the Los Alamos Scientific Laboratory (LASL) required a new pulsed-power supply to drive the gas discharge. Analysis of the system showed that the most cost-effective approach to the pulsed-power supply design was a single-mesh pulse-forming network using twenty-four 1.2-MV, 300-kJ Marx generators, each with an inductance less than 3 μH.[1] None of these parameters was considered beyond the state of the art. However, in the event of a short circuit on the output, caused, for example, by an output-cable failure, the circuit would ring with high reversal, giving a peak current of 400 kA, with charge transfer of 6 C. Because this peak current would push the state of the art in pressurized spark-gap technology, a spark-gap development program was instituted. A spark-gap prototype was run for 2000 shots without maintenance under conditions (500 kA, 10 C) even more severe than the Marx short-circuit conditions. This program is described in detail in Appendix A. Table I shows the Marx specifications.

TABLE I
MARX SPECIFICATIONS

Open circuit voltage	1.2 MV
Load voltage	550 kV
Stored energy	300 kJ
Inductance	<3 μH
Load current, charge	250 kA, 1 C
Short-circuit current, charge	400 kA, 6 C
Prefire rate	<0.001
Jitter, rms	<20 ns
Reliability	>0.999
Maintenance schedule	1000 shots

A Marx design was selected which we felt would meet these specifications. The capacitor chosen was the 2.8-μF, 60-kV, castor-oil-impregnated paper design which was life tested for the Scyllac program. To give the voltage and energy required, 3 of these are used in parallel and 20 in series. Bipolar charging produces a 120-kV spark-gap voltage. A double-folded geometry,

with the capacitor terminals facing each other and the spark gaps between (Fig. 1a), was selected to give the required inductance. Figure 1b is a close-up of the spark-gap region. By operating the spark gaps with a high safety factor (far below self-breakdown), we felt that the prefire rate would be low, while good trigger coupling would still give low jitter.

A prototype of the Marx was built so that the design concepts could be tested, and reliable electrical and mechanical components could be developed. Partway through the testing program, we decided that the Marx generator system should be built by a contractor because of limitations on in-house engineering personnel. Although the contractor chose a different geomety for the Marx, the testing program provided valuable information, which later was used by the pulser contractor.

II. SUMMARY OF RESULTS

A full-sized prototype was built and discharged a few thousand times into a dummy-load resistor. We measured primarily the Marx inductance, the trigger delay jitter, and the prefire rate. The results of these tests are discussed in this section; more detailed discussion and other information gathered during the testing are given in Sec. IV.

The inductance was measured by short-circuiting the load resistor with a sheet of copper and firing the Marx with low charge voltage (15 kV). The inductance, which may be calculated from the ringing frequency, was found to be ~2.4 μH. However, we concluded from the full-voltage tests that the high-voltage bus bar on the capacitor should be spaced a little farther away from the capacitor case. This additional space and the inclusion of the cable terminations will add ~0.3 μH, making the total inductance ~2.7 μH.

We measured the trigger delay jitter, using the output signal from a single-turn B-dot loop to trigger the stop gate on a digital time interval counter. The start could be triggered from anywhere in the trigger chain. Most measurements were made with the start signal tapped off the output from a 350-V solid-state trigger generator. The trigger system is described in detail in Sec. IV.B. The trigger system output is a four-stage Marx charged to 40 kV/stage, driving three 30-ft cables, connected to the

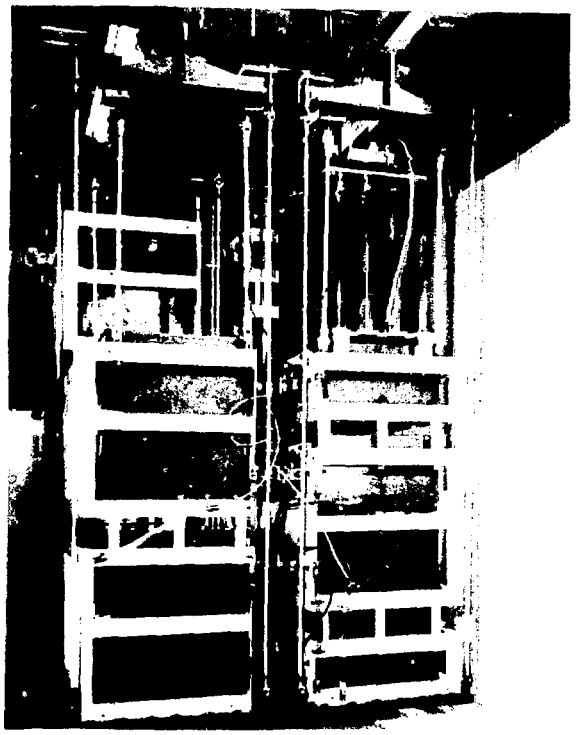

Fig. 1a.
Prototype 300-kJ Marx generator.

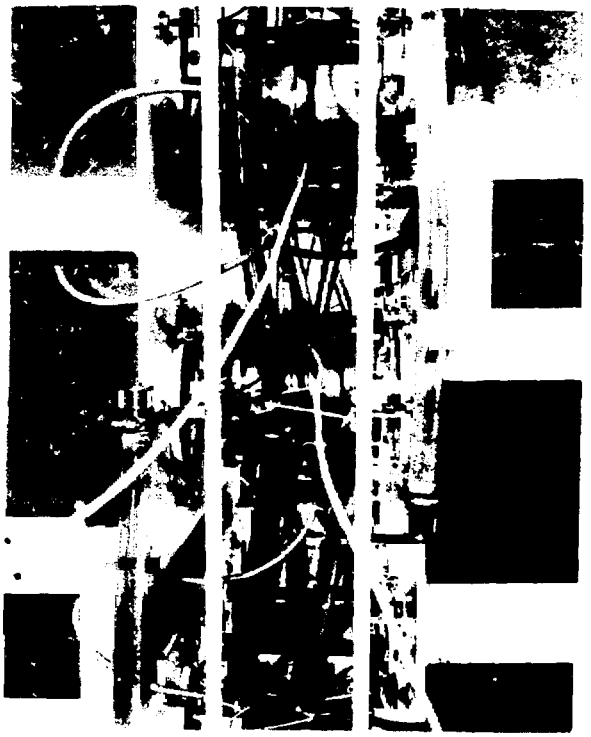

Fig. 1b.
Close-up of spark-gap region.

first three gaps through liquid resistors. Jitter was measured with charge and trigger coupling resistors made of either liquid or Carborundum. No significant difference in jitter was found between these two cases; for both, the rms jitter is ~12-15 ns.

The prefire rate was at first excessive, on the order of 0.01. Previous experience had indicated that the use of a fine mesh (10 μm) filter on each spark gap would significantly affect the prefire rate. This was confirmed when the addition of these filters decreased the prefires to 3 in a 1000-shot series.

III. MARX DESIGN

A. Marx Geometry

The Marx design is determined primarily by the voltage, energy, and inductance requirements. For reasons detailed below, the capacitors used are 2.8-μF, 60-kV rated, storing 5 kJ each. We need 20 in series to give the required voltage and 3 in parallel at each stage to give the required energy. The inductance specification (less than 3 μH) is low, but not beyond the state of the art. We decided to approach the problem of design for inductance by modeling rather than analysis. Capacitors of the same physical size and inductance as those to be used in the Marx were laid out in various arrangements. Spark gaps were simulated by brass tubes for the electrodes and wires for the arcs. The capacitors were all charged in series and switched with a single spark gap into a short circuit. The inductance was calculated from the ringing frequency.

Possible Marx geometries of progressively lower inductance may be classified as one-dimensional (linear), two-dimensional (single-folded), and three-dimensional (double-folded) (Fig. 2). A 1.2 MV linear Marx, with the current return 12 in. from the capacitors (to allow for 6 in. of insulation and a 6-in.-diam spark gap), has about 5 μH. A single-folded Marx, with 6 in. between the folds at the high-voltage end tapering to zero at the fold point, with the spark gaps coming out of the plane of the Marx, and with one capacitor per stage (Fig. 3), gave 3.75 μH. A model of the double-folded geometry (Fig. 1), with two parallel capacitors per stage, with 13 in. between capacitor faces, and with 11 in. between the high- and low-voltage stacks, gave 2.7 μH. Alternative ways of folding did not make a significant difference, that is, all single-folded geometries with equivalent spacings gave about equal inductance.

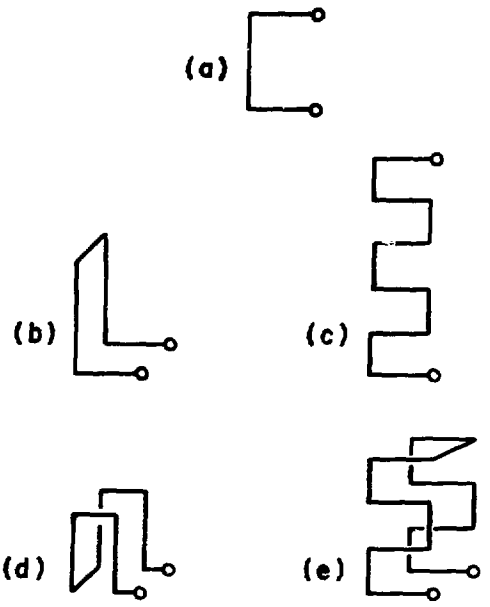

Fig. 2.
Some possible Marx generator current paths: (a) linear; (b) and (c) single-folded; and (d) and (e) double-folded.

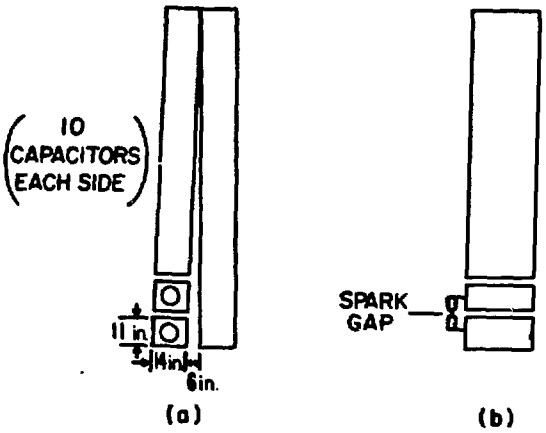

Fig. 3.
Mockup of single-folded Marx: (a) top view (spark gaps not shown); (b) side view.

We concluded that a double-folded geometry is required to meet the inductance specification. The choice then remained whether to put the spark gaps on the inside of the Marx, with the capacitor headers facing each other, or to put the spark gaps on the outside, with the headers facing out. We chose to put the spark gaps on the inside (Fig. 1) in order to leave the outside of the

Marx very clean, thus reducing breakdown problems and allowing the tank walls to be closer to the capacitors. The penalty, which we discovered is a major one, is that the spark gaps are very difficult to service. The Marx system contractor has chosen to put the spark gaps on the outside.

B. Marx Circuit

The Marx circuit involves the connections and values of the charge resistors and trigger resistors, coupling to the trigger system, coupling to the charge system, and the dump circuit. The design of the Marx circuit has a profound effect on the performance of the Marx generator.

The first decision usually made in the design of a Marx circuit is the charge mode. Unipolar charging requires as many spark gaps as series capacitors, but the spark gaps are only required to hold off the capacitor charge voltage. Bipolar charging requires only half as many spark gaps, but each is required to hold twice the charge voltage. If symmetrical midplane triggered spark gaps are used, bipolar charging also has the advantage that the trigger electrodes are at zero potential and may be biased by connection to a capacitor case down the Marx. Bipolar charging was chosen for this design because the spark-gap voltage (120 kV) was not excessive (similar spark gaps at Sandia National Laboratories operate at 200 kV),* inductance was lower with fewer spark gaps, and we believed costs would be lower because the spark-gap unit cost is not a strong function of voltage.

The interstage stray capacitance (Fig. 4) in designs (c) and (e) (Fig. 2) will aid in triggering by doubling the spark-gap voltage during Marx erection.[2] The charge resistors also may be used to aid in the Marx triggering by coupling alternate stages. In this case, with bipolar charging and the double-folded geometry, the mechanically convenient resistor connection scheme (Fig. 5) gives the same voltage multiplication as the stray capacitive coupling, that is, the charge resistors neither discharge nor charge the stray capacitance.

Because the charge-coupling resistors are neutral with respect to the stray capacitive coupling, the RC time is not important and does not determine the resistor value. The resistor value is determined by the self-decay time of the Marx as a lower limit. With stage capacitance on the order of microfarads, and discharge time of a few microseconds, the effective resistance must be tens of ohms. There are six strings in parallel, so each resistor must be about 100 Ω or more. Since the charge-coupling resistors are included in the trigger circuit for the upper stages, the value must be as low as possible to enhance

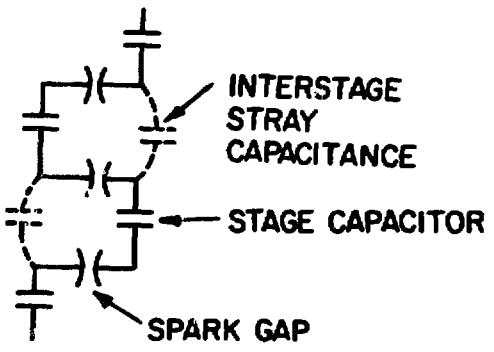

Fig. 4.
Interstage capacitive coupling.

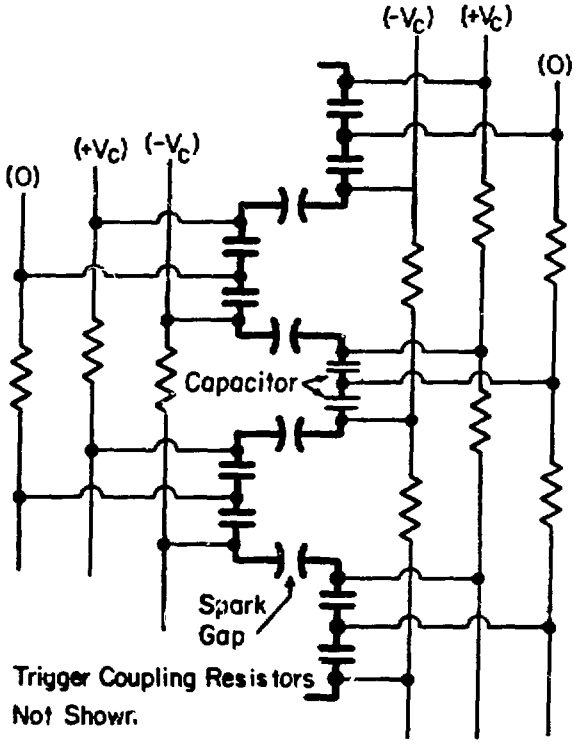

Fig. 5.
Charge coupling schematic.

*T. H. Martin, Sandia National Laboratories, furnished this information.

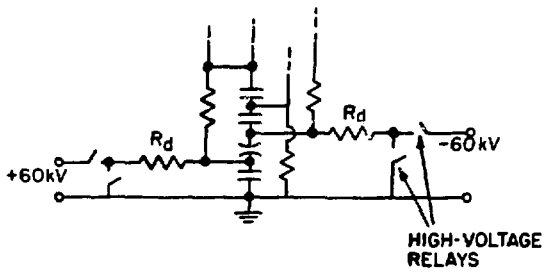

Fig. 6.
Charge/dump circuit.

low jitter operation. Hence, 100 Ω was chosen as the stage charge-coupling resistor.

The charge/dump circuit is shown in Fig. 6. The resistor R_d provides both isolation of the power supply from the Marx and an energy dump for the Marx if it is charged and the decision is made not to operate the laser. This resistor must be made large enough (thermally) to absorb most of the Marx energy. The resistor value should be made large compared to the stage resistors so that the majority of the energy is dissipated in the dump resistor. The value of the dump resistor is 5000 Ω. It is made up of a series-parallel combination of twenty 1000-Ω, 225-W, Dale Electronics, Inc., wire-wound resistors. We found, experimentally, that each resistor can dissipate 10 kJ in a few seconds without damage.

Low-jitter operation of the Marx is achieved by coupling the upper stage trigger electrodes down the Marx to a point which is at ground during charging. The trigger electrode may be coupled either to a trigger electrode further down or to a capacitor case. The further down the Marx the trigger electrode is coupled, the higher the relative voltage between the trigger electrode and the main electrode as the Marx erects and, consequently, the lower the jitter should be. Coupling down to other trigger electrodes is common but the external trigger applied to the first gaps is also coupled to the upper gaps [Fig. 7(a)]. Consequently, jitter may be high because the erection mode will depend on which gaps break first. Coupling to capacitor cases down the Marx, as in Fig. 7(b), may still cause anomalous modes, but they are less probable and, therefore, jitter should be lower. This trigger-coupling scheme was the one chosen. The number of stages down to connect the trigger electrode is a compromise between the voltage holdoff required of the trigger coupling resistor and the reduced jitter to be gained through increased trigger drive. The

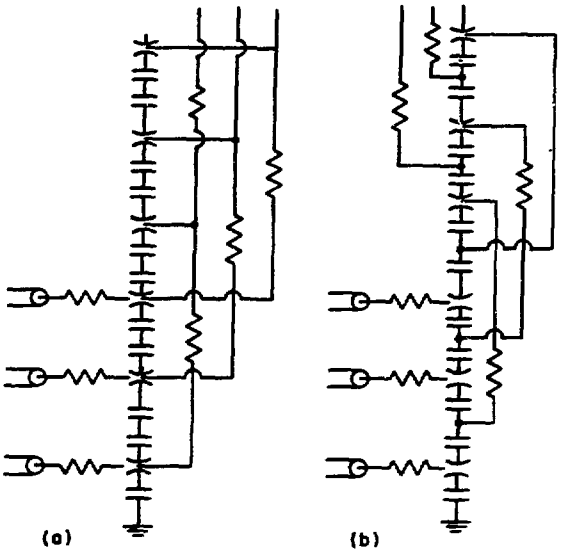

Fig. 7.
Upper stage trigger electrode coupling circuits.

coupling shown drives the trigger electrode to −300 kV with respect to the positive main electrode. The self-breakdown voltage of this half of the gap is 120 kV. Breakdown should be rapid with low jitter.

C. Spark Gaps

The spark gaps must carry the full discharge current and charge. For normal discharge conditions, these are about 250 kA and 1 C. In the event of a prefire, a shunt relay on the Marx output with a 3/4-Ω dummy-load resistor will limit the load voltage to about 300 kV. The spark-gap duty is then about 350 kA with 2 C charge transfer. Under short-circuit conditions resulting from a cable breakdown or Marx-to-tank arc, with only the arc resistance, internal resistance, and inductance of the Marx to limit the current and damp the ringing, the spark-gap duty is over 400 kA with more than 6 C. This is severe for a single-channel, high-pressure spark gap. To provide a reliable system, we felt that a spark-gap protoype should be able to handle 1000 shots under short-circuit conditions without maintenance.

The most convenient switch for use in a low-jitter Marx generator is a midplane-triggered three-electrode spark-gap. If bipolar charging is used, then a symmetrical gap is preferred because proper bias of the

trigger electrode is achieved by tying it to a ground point during charging.

To have a wide operating voltage range, the spark gaps must either operate at high pressure, or use a high breakdown strength gas at maximum charge voltage. The most commonly used switch gases are dry air and sulphur hexafluoride (SF_6). Because SF_6 absorbs 10.6 μm radiation, it is best not to use it in a CO_2 laser facility; therefore, it is necessary to use high-pressure air. The gaps must be pressurized to 10 psig (21 psia) minimum to keep out oil. (Atmospheric pressure in Los Alamos is 11.2 psia.) With 10 psig used at 20-kV charge, then at 60 kV, the pressure must be 52 psig (63 psia) if voltage holdoff is linear with pressure.

To keep the prefire rate low, the gaps should be run with a safety factor as high as possible relative to the mean self-breakdown voltage. Because the gap voltage in the upper stages is doubled by stray capacitive coupling, a safety factor of 2 seemed reasonable, considering that low jitter is required and that jitter is a strong function of spark-gap safety factor and trigger voltage. If jitter had been too high, we either could have coupled the trigger electrodes farther down the Marx or could have reduced the safety factor.

The spark-gap geometry (Fig. A-1) was chosen because it uses simple shapes: flat metal end plates, flat trigger electrode, hemispheric main electrodes, and cylindrical insulators. The dimensions are determined by inductance and weight. Appendix A describes a spark-gap development program which meets all the requirements.

D. Capacitors

The choice of capacitors depends on other elements that are voltage dependent, most notably spark gaps. As mentioned above, voltages up to 100 kV are acceptable because these are used in the Marx generators in the Hydra-Proto-EBFA systems at Sandia National Laboratories.* The choice also depends on the total Marx energy, Marx voltage, and the number of capacitors in parallel. The complexity of the hardware increases with the number of parallel capacitors. The Marx energy required is 300 kJ at 1.2 MV. The energy per stage is 300 kJ divided by the number of stages (Fig. 8).

Because low-voltage capacitors are more efficiently constructed than high-voltage capacitors, they offer

*T. H. Martin, Sandia National Laboratories, furnished this information.

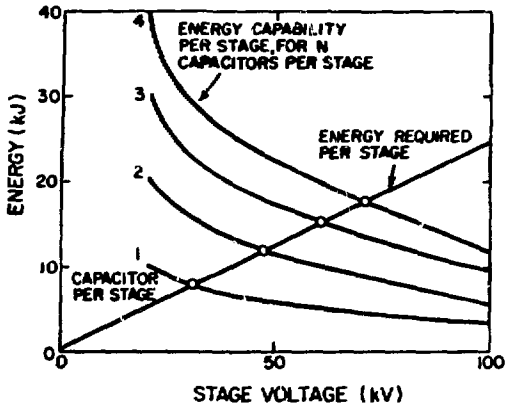

Fig. 8.
Energy per capacitor and energy per stage vs stage voltage.

higher energy per capacitor. At the time this Marx generator was being designed, available life-tested capacitors were 10 kJ at 20 kV, 5 kJ at 60 kV, and 3 kJ at 100 kV. The resulting stage energy using one, two, three, and four capacitors in parallel is plotted in Fig. 8. This figure shows that one could use one 30-kV, 8-kJ capacitor per stage, two 50-kV at 6 kJ each, three 60-kV at 5 kJ each, or four 70-kV at 4.5 kJ each. Of these, only the 5-kJ, 60-kV capacitors actually have been built and life tested. Even though the others lie on the curve of energy vs voltage established by tested capacitors, a life-test program would still be required. For this reason, the 60-kV, 5-kJ (2.8-μF) capacitor was chosen as the energy storage unit. Short-circuit testing of this capacitor is described in Appendix B.

We considered developing even higher energy-density capacitors so that fewer parallel capacitors would be required. For example, we estimated that possibly up to $500 000 could be saved by using 60-kV, 4.2-μF capacitors. However, the cost of proving the reliability of these capacitors would be several hundred thousand dollars and might not have resulted in a useful capacitor.

E. Resistors

Many Marx generators are built using liquid charge-coupling resistors (aqueous solutions of copper sulfate, sodium chloride, etc., in a plastic tube with metal electrodes) because they are easily built, have high-voltage holdoff capability, and are capable of high

energy dissipation (tens of joules per cm^3). However, liquid resistors also have a tendency to leak, which can be reduced but never completely eliminated.

On the other hand, several types of solid resistors are available. Carbon composition resistors, manufactured by Carborundum Co., and high-power wire-wound resistors were tested for voltage holdoff and energy dissipation capability. The results are described in Appendix C of this report. As a result of these tests, coated Carborundum resistors were chosen for use in the Antares Marx generator prototype.

F. Mechanical Design

With three capacitors in parallel and bipolar charging, the capacitors may be grouped in a set of six with their cases connected electrically. We thought that the most convenient way to group the capacitors was to support them in racks. The ground connection on these capacitors is a stiff ring with threaded holes. The high-voltage terminal is coaxial with the ground ring. The rack has a metal plate on the front, with six holes for the capacitor high-voltage insulators. The capacitors are attached to the plate by bolts through holes in the plate into the threaded holes in the ground ring. A box frame completes the rack, providing support for the back of the capacitor and the Marx column. Figure 9 is a photograph of the partially assembled Marx showing the capacitors in the racks. Details of the design may be found in LASL Dwg. 89Y-61701-E6.*

The capacitor racks are supported by long fiber glass reinforced epoxy rods which are glued into a steel clevis on both ends. The rods are manufactured by several companies, including Permali Inc. and Nupla Corp. They are used to support the bottom capacitor racks from above. The upper racks are then supported by stacking, with nylon spacers between racks. Details may be found in LASL Dwg. 89Y-61724-J1.*

The high-voltage terminals of the three parallel capacitors are connected by a bus bar made of 1/8-in. by 2-in. aluminum. The spark gaps are supported by a flexible bar at each end, so that any misalignment or motion of the capacitor stacks will be taken up by the bus bar without excessive force on the capacitor terminals or spark gaps. The bus bars are detailed in LASL Dwg. 89Y-61701-D8.*

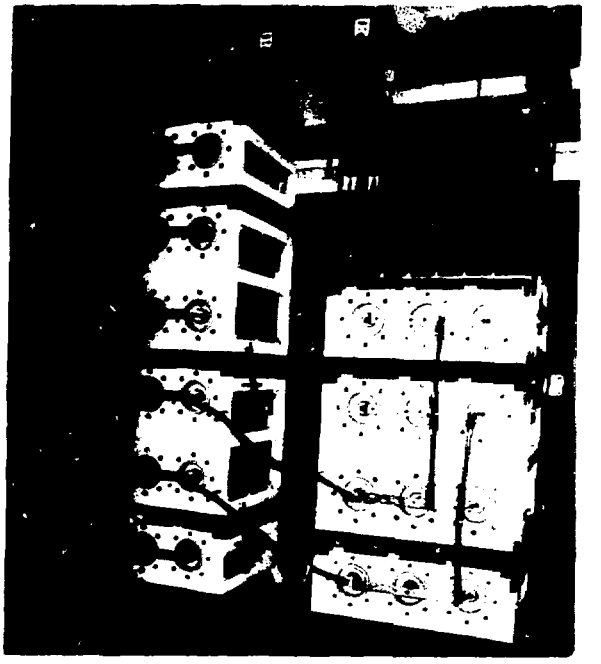

Fig. 9.
Partially assembled Marx generator with capacitors in racks.

G. Spacings

The Marx inductance is determined by the geometry and by the spacings, which depend on the required voltage. There are three major voltage holdoff spaces: from bus bar to capacitor rack (60 kV dc), spark gap end-to-end (120 kV dc), and between the Marx input and output (600 kV pulse).

The bus-to-rack spacing determines the inductance of the system of parallel capacitors. Although this is not a major portion of the Marx inductance, the spacing should not be made excessive. For the prototype, this spacing was made adjustable so that the optimum spacing could be determined. A mean stress of about 40 kV/in. was used as a starting point for the design.

The spark-gap length, which is determined by tracking of the inside surface during use, specifies the spacing between opposing columns of the Marx. Testing of the

*These drawings are available from LASL group L-10, Mechanical Section, Bldg. 186.

spark gap, described in Sec. IV.D., determined that an acceptable length was 8 in.

The space between the high-voltage terminal and the low-voltage column must hold the Marx output voltage, plus any overshoot caused by impedance mismatch. Because the output stage is not lined up opposite the ground stage, but is a few stages down, the peak voltage to be held is about 600 kV. The holdoff strength of oil for microsecond pulses is about 250 kV/in., so a working stress of 125 kV/in. is acceptable. A spacing of 4.75 in. was used. For added safety, a larger spacing was used at first, but 4.75 in. was required to reach the inductance goal.

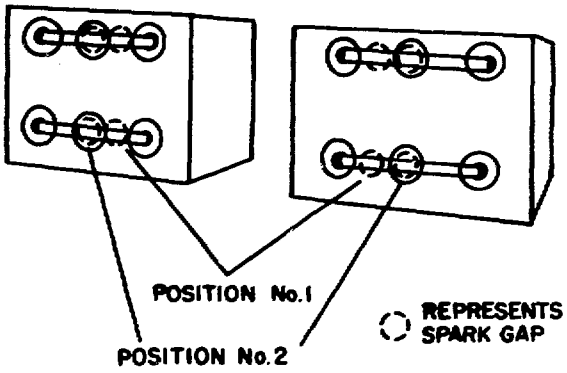

Fig. 10.
Spark-gap positions.

IV. MARX TEST RESULTS

The Marx prototype was built in the summer of 1977, and testing continued until July 1979. As a result of these tests, some major changes were made in the design. Finally, in July 1979, 1000 shots were fired at full charge voltage with no failures. The goals of inductance, jitter, and reliability were met, and we came close to meeting the prefire rate goal.

A. Inductance

The Marx inductance was measured by shorting the dummy-load resistors with a copper sheet, firing the Marx at low-charge voltage (±15 kV), and measuring the ringing frequency on an oscilloscope trace.

We started out with 18 in. between the high-voltage and low-voltage columns for convenience in assembly rather than voltage holdoff. The inductance was 3.7 μH. When the spacing was reduced to 4 in., the inductance was 2.7 μH. These measurements were made with the spark gaps positioned as shown in Fig. 10, position No. 1. Figure 9 clarifies the relationship of the racks. When the spark gaps were put in position No. 2 (farther apart), the inductance was reduced to 2.4 μH. It did not seem, intuitively, that the reduction should occur, but apparently the closer connection to the outer capacitors compensates for the increased distance between spark gaps.

B. Jitter

To achieve a sufficient degree of simultaneity among the 24 Marx generators, the Marx jitter goal was 20 ns or less. The Marx design used capacitive and resistive coupling between stages to over-volt the gaps during Marx erection and coupling of the trigger electrodes to lower stages to speed the breakdown.

The jitter is found by measuring the time delay between the initial low-level trigger and some signal that is characteristic of completion of Marx erection and by calculating the standard deviation of a set of time delays. Because the output voltage and current both rise to peak in about a microsecond, these signals will not be useful for accurately measuring times with a resolution that is small compared to 20 ns. A signal proportional to dI/dt will have a short risetime, so a dI/dt probe was placed at the ground end of the Marx. The noise problems were severe. Even with a Tektronix 507 oscilloscope in a double-shielded room, with the signal lead run through a copper pipe, and with a shielded Rogowski loop, the initial rise in the signal was buried in noise. Since the Antares control system will use fiber-optic coupling for signals, equipment was available to make a fiber-optic-coupled analog signal system. This relieved the noise problems, although some dV/dt coupling was

apparent if the probe was not well shielded. A single-turn loop was used as the dI/dt probe.

The system used to trigger the Marx for the jitter tests had an output voltage of 160 kV. The final amplifier was a four-stage Marx, using Pulsar Associates, Inc. SW-50 K, self-illuminated spark gaps. The four-stage Marx had jitter of less than 5 ns. The four-stage Marx was triggered by a PATCO PT-55 spiral-line generator, which in turn was triggered by a PATCO PT-70, a solid-state device which requires a 10-V driving pulse and has 1/2-ns jitter. Jitter was measured from the PT-70 output monitor to the gas pulser output pulse.

A Hewlett-Packard Co. 5370-A digital time delay counter was used to measure the time delays. The start signal for the counter came from the PT-70 monitor and the stop signal from the dI/dt probe.

The first jitter measurements on the Marx prototype were made before the Carborundum charge resistors were installed in the Marx, while the liquid resistors were still being used. We felt that this configuration might give lower jitter because of the capacitance of the liquid resistors. Jitter was calculated for sets of 25 shots and was about 11.5 ns, with the gaps operating at a safety factor of 2.0. After we installed the Carborundum resistors, the jitter was about 14.5 ns. This change in jitter is probably not significant because it could be due either to the change in Marx configuration or to a change in the instrumentation.

C. Prefire Rate

The Marx prefire rate may have a large impact on the total system reliability. Typical large Marx prefire rates are ~0.01. Twenty-four Marx generators would cause a system prefire rate of one shot in four. We hoped to decrease the prefire rate to 0.001 by operating the spark gaps with a self-breakdown safety factor of 2.0 (one-half of self-breakdown voltage), if this turned out to be compatible with the jitter requirement (as safety factor is raised, jitter will increase). Although the jitter was acceptable, the prefire rate in the initial tests was about 0.01. Because there were also problems with spark-gap insulator tracking, which were attributed to insufficient airflow in some of the spark gaps (see Sec. D on spark-gap testing), the air system was changed from that in Fig. 11(a) to 11(b). In Fig. 11(a), the gaps are connected in parallel to the airflow system, but the flow

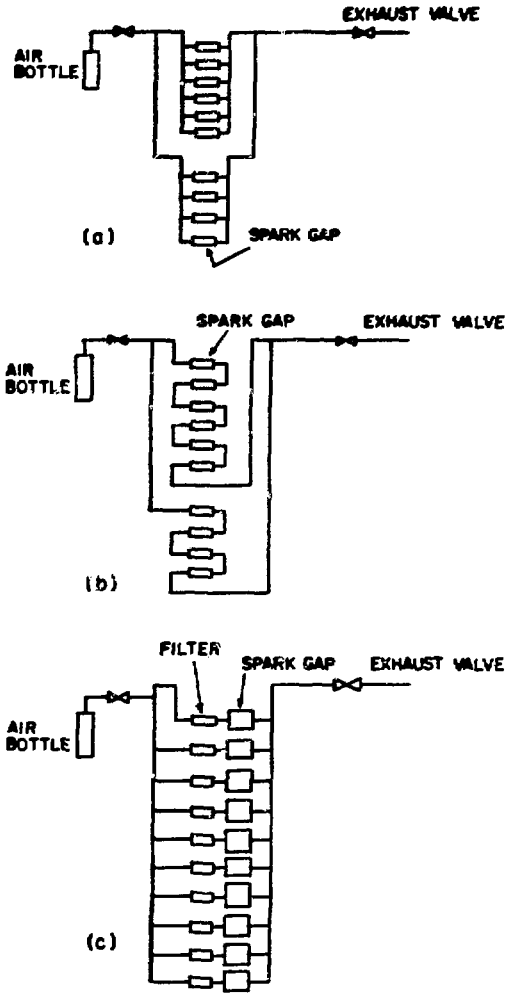

Fig. 11.
Airflow systems.

impedances are not equal; therefore, the gaps at the end of the chain get much less airflow. In Fig. 11(b), sets of gaps are in series so that they get equal airflow. This did not help the prefire rate. The airflow system was then changed to that in Fig. 11(c), in which a manifold is used to feed air to each spark gap separately. Air filters with 10 μm mesh were used to ensure that no dust or air-line particles were blown into the gap. These filters restricted the flow to 8 scfm per gap at 50 psig. The gaps were flushed for 0.5 min. The result, a series of 1000 shots with 3 prefires, was a large improvement and was considered acceptable.

D. Spark-Gap Testing

During the initial testing using the airflow system in Fig. 11(a), one of the spark gaps developed a conducting track on the inside surface of the insulator after about 250 shots. This was surprising because the spark-gap prototype had run 2000 shots under short-circuit conditions without maintenance. The greatest observable difference was that the gap prototype had been flushed after each shot for 10 s at 3.3 cfm. The flow rate in the Marx was 8 cfm, but the flow was not equal to all gaps because of longer lines to the gaps near the bottom of the tank. We found that the gaps near the bottom of the tank had a sticky coating on the inside insulator surface, while those near the top were drier. We attempted to solve this problem by using the airflow system in Fig. 11(b), in which the gaps are connected to the airflow system in series to ensure equal airflow to each gap. We then ran 500 shots before tracking another insulator, but there was still a sticky coating on the insulators. A gas manifold system was then installed to ensure equal airflow to each spark gap. The airflow was 8 cfm to each gap for 0.5 min. We were then able to run 1000 shots without problems. The gaps were then disassembled and inspected. The insulator surfaces were dry and showed no evidence of tracking. Apparently, the air-breakdown products, most likely the ozone, when not sufficiently flushed from the spark gap, react with the nylon insulator to form a conducting coating which eventually carries enough current to heat and carbonize the nylon.

E. Oil Breakdown

There were no problems with pulse breakdown of the oil during the approximately 2000 full-voltage discharges of the Marx. The highest stress was between the input and output stages of the Marx, where a voltage of about 550 kV is held across 10 cm.

There were a few instances of dc breakdown during charging of the Marx. Some of these occurred during the phase of testing when liquid charge resistors were used. Spacings were tight and the resistors were difficult to hold in place. The place where the breakdown occurred was never found; the only evidence was a broken resistor. There was one instance where breakdown occurred from a high-voltage bus bar (which interconnects the capacitor high-voltage terminals in a stage) to the capacitor rack. The breakdown was actually from a spark-gap mounting screw, which extended about .25 in. through the bus bar. The spacing from the end of the screw to the face of the capacitor rack was 1.25 in. The end of the screw was very sharp. The high field was eliminated by reversing the screw so that the head faced the capacitor rack on all the spark-gap mountings. No other oil breakdowns occurred. If this Marx design were to go into production, we would increase the spacing by .25 in.

F. High Current Contacts

Because of the high current, care must be taken at all pressure contacts to prevent sparking. Soft-copper washers were used at all such places, except between the capacitor ground ring and the face of the capacitor rack. Here, insertion of washers during assembly proved very difficult. We incorrectly assumed that, because of the large area involved, there would be sufficient contact to prevent sparking, but there was enough sparking to cause a significant amount of carbon (caused by oil decomposition) to diffuse out and across the capacitor terminal. This was the probable cause of two capacitor bushing flashovers. The solution to this problem would be to use either copper gaskets or thinner plate for the front face of the capacitor rack.

G. Spark-Gap Variability

The spark gap tolerances were chosen so that the maximum build-up of tolerances would affect spark-gap spacing (and presumably self-breakdown voltage) by 10%. After the spark gaps were assembled, the self-breakdown voltage of each side of each gap was measured at atmospheric pressure with a small airflow. A 2.4 nF capacitor was connected across the half of the gap being tested, and a few hundred shots were run to condition the gap. The relative standard deviation of breakdown voltage was 1.8%. The largest deviation from the mean was 3.4%. This test gave us confidence that spark-gap variations would not contribute to the prefire rate.

The measured self-breakdown voltage of a spark gap that had run 500 shots was 5% lower (6 kV at 120 kV) than that of a new gap.

REFERENCES

1. K. B. Riepe and J. Jansen, "Pulsed Power Systems for the LASL High Energy Gas Laser Facility," Proc. - IEEE Int. Pulsed Power Conf., Lubbock, Texas, November 9-11, 1976, IEEE document 76CH1147-8RE65.

2. R. A. Fitch, "Marx- and Marx-like High-Voltage Generators," Fourth Symposium on Engineering Problems of Fusion Research, Washington, D. C., April 20-23, 1971, IEEE Trans. Nucl. Sci., Vol. NS-18, No. 4, August 1971, pp. 190-198.

APPENDIX A

SPARK-GAP DEVELOPMENT

I. INTRODUCTION

The Antares Laser Fusion Project at LASL requires the use of twenty-four 1.2-MV gas-pulser Marx generators, each using ten 120-kV, 250-kA, 1-C spark-gap switches. Each switch must function with a negligible prefire rate and a maximum jitter of less than 10 ns over an operating range of 40 to 120 kV and exhibit no significant change in its characteristics for at least 10 000 pulse operations. The switch must be designed to survive a minimum of 2000 faults, which would occur when the gas pulser arcs to ground as the result of a cable failure or a breakdown in the laser gas.

Space restrictions in the gas-pulser oil tank and the need to keep the circuit inductances to a minimum require that the shape and size of the switch approximate a right-circular cylinder 25 cm by 25 cm or smaller.

We did not intend originally to implement a spark-gap development program at LASL. Three designs were purchased from three different high-voltage equipment manufacturers on a best effort basis against a worst case fault specification of 400 kA, 5 C, 120 kV, M = 2 (safety factor), and with operation under mineral-base transformer oil. The testing of each design against these specifications was performed at LASL.

None of the purchased spark gaps tested was successful. Each submitted design was lacking in mechanical impact strength, and optimum materials were not being used in the fabrication of electrodes and electrode holders. The best aspects of each design were combined or modified to arrive at a workable spark gap.

The basic configuration chosen from the preliminary testing was similar to that shown in Fig. A-1. This configuration was preferred because of its inherent mechanical simplicity. Subsequent extensive testing and modifications produced a switch with mechanical structure adequate to survive 2000 simulated fault operations. A special copper-tungsten composite material, Plansee K25, used for the fabrication of the electrodes, significantly extended their life. Tests at normal operating conditions were performed to characterize switch jitter as a function of operating voltage, gas pressure, and trigger voltage. Although SF_6 gas was initially tried as a dielectric and purging gas, dry breathing air was found to be more satisfactory and was used throughout all subsequent tests.

II. FINAL SPARK-GAP DESIGN AND TEST RESULTS

A. Final Design

The completed spark-gap design, which evolved from many trial-and-error modifications, is shown in Fig. A-1. This switch has been tested for 2000 worst case fault operations with no measurable deterioration in performance.

The main electrodes are hemispheres 5 cm in diam. The air gap spacing is 2.79 cm. The trigger disk electrode is 0.64-cm thick, 10.2-cm diam, with a 2.5-cm-diam center hole. The edge of the trigger disk center hole is machined with a full radius.

B. Fault Test

The completed prototype was subjected to 2000 consecutive operations to simulate a fault condition in the Antares Marx generators. A schematic diagram and associated test parameters are shown in Fig. A-2. Fault-test waveforms are shown in Fig. A-3. A 120-kV,

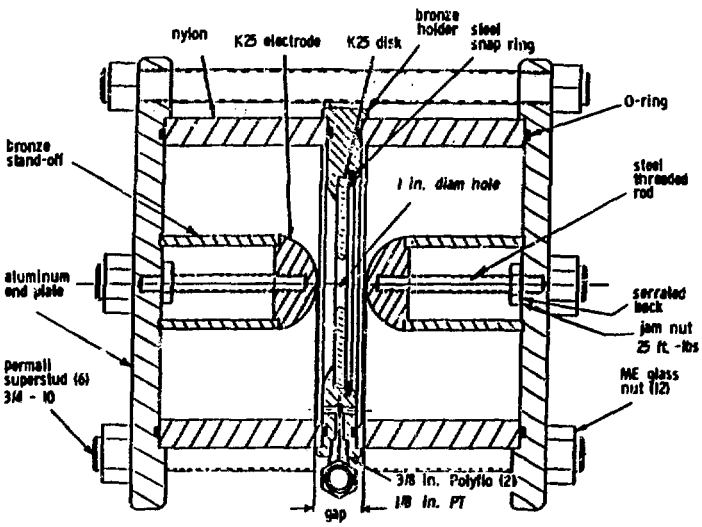

Fig. A-1.
Tested spark-gap design.

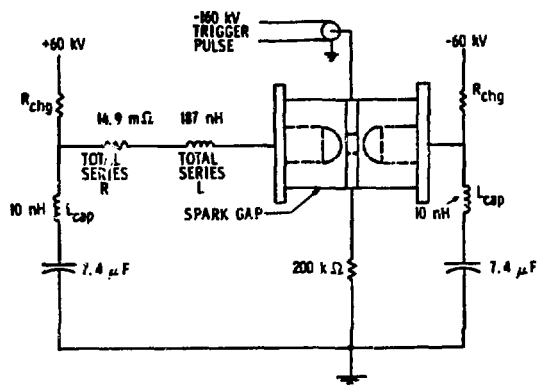

I (peak)	= 482 kA
V holdoff	= 120 kV
q per shot	= 9 C
Energy switched	= 27 kJ
f (ring-down)	= 182 kHz
Repetition rate	= 1 shot/min

See Fig. A-3 for the resulting waveforms.

Fig. A-2.
Worst case fault-test parameters.

27-kJ capacitor bank was switched with minimum circuit impedance, resulting in an oscillatory ring-down through the spark gap. This test generated a peak current of 480 kA, 9 C per shot at 120 kV, a ringing frequency of 180 kHz, with a repetition rate of one shot per minute. The gas pressure (air) was adjusted so that self-breakdown would occur at twice the operating voltage, creating a safety factor of M = 2.

The switch was purged with dry breathing air immediately after each shot. Purge duration was 10 s at 3.3 cfm (0.055 ft^3/s), resulting in 1.7 mass-volume changes. Brass was used for the trigger disk holder, and the trigger disk electrode was fastened with peened screws machined flush with the holder surfaces.

C. Fault-Test Results

After 2000 shots, the switch was removed from the test fixture and examined. The 5-cm-diam K25 electrode hemispheres showed insignificant wear. Black and brown surface discoloration and roughness were present indicating formations of oxides.[1] Cleaning the oxides from the surfaces revealed small amounts of surface pitting but no grain boundary erosion or cracks.

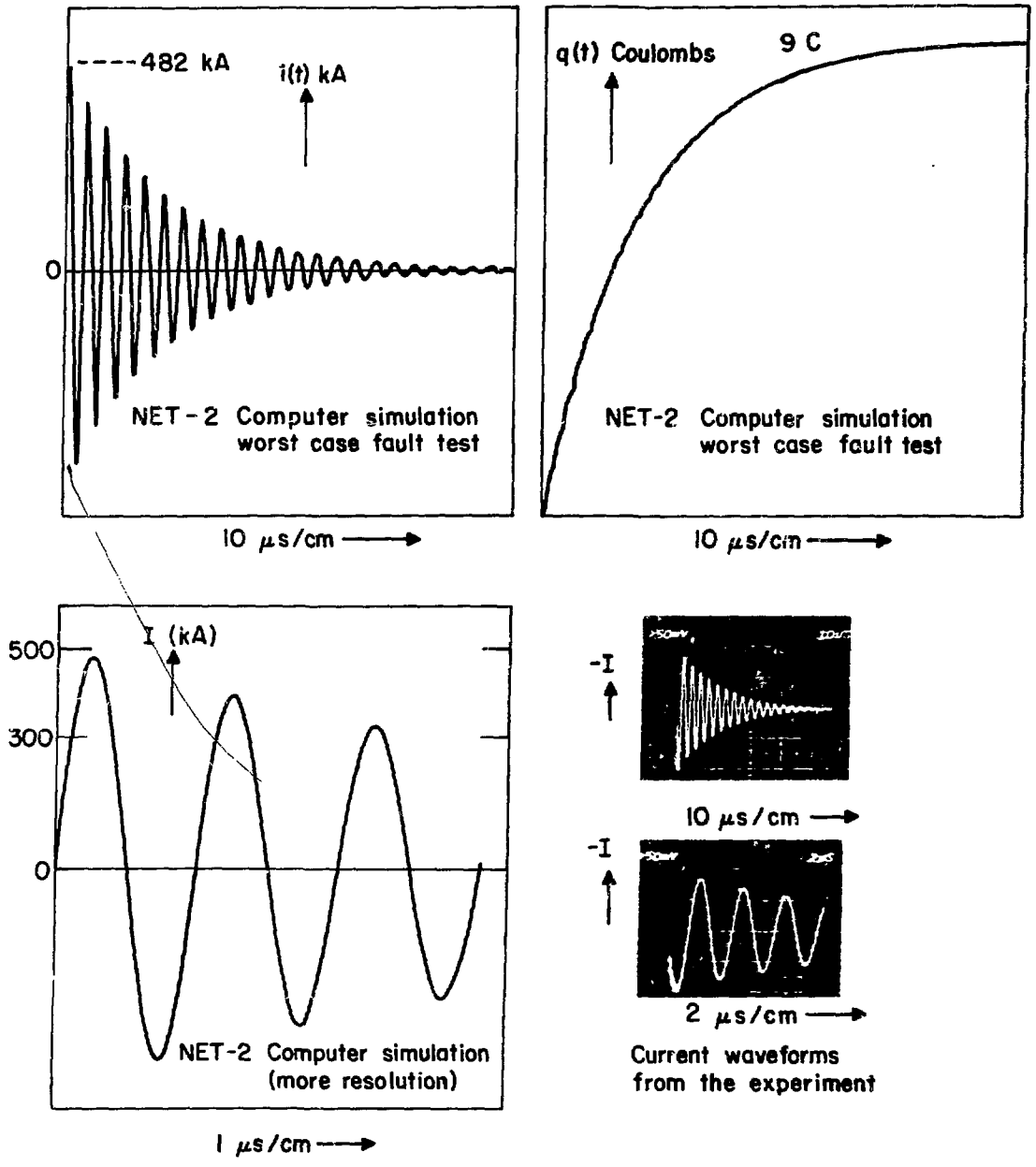

Fig. A-3.
Worst case fault-test waveforms.

Changes in the physical dimensions of the hemisphere were negligible. The K25 trigger disk, 0.64-cm thick by 10.2-cm diam with a 2.5-cm-diam center hole, exhibited marked erosion. The hole had not enlarged. Preferential erosion was evident on a section of the surface oriented toward the negatively charged half of the capacitor bank. This erosion was in the form of localized pitting approximately 0.01-cm to 0.03-cm deep over an area of approximately 1 cm^2 near the hole edge. The same oxide discoloration and roughness were present as appeared on

the hemispheres. The initially negative-oriented surface showed slightly more wear. Scattered small pits and discoloration indicated minor arc impingement on the brass trigger disk holder.

The interior surfaces of the nylon insulator were discolored, glazed and rough, but no cracks, burns, or electrical tracking were in evidence. It appeared as though heat had glazed the nylon, short wavelength radiation had discolored it, and hot, nonconducting metal oxide had splattered and fused onto the surfaces, resulting in a rough but physically durable coating. Blue-colored powder (probably zinc oxide) had settled by gravity on the lower halves of each insulator. At the conclusion of the 2000-shot test, the dielectric strength of the nylon's surface was still sufficient to hold off 120 kV and M = 1.2. The full voltage (120 kV) was applied to the gap for 3 min with the dielectric gas pressure at 30 psig. There were no occurrences of self-breakdown or surface tracking. This test was repeated three times with several full-power shots interspersed between the 3-min holding periods.

D. Normal Operating Conditions

The normal operating waveform for the switch in the gas pulser is shown in Fig. A-4 and a NET-2 computer simulation is shown in Fig. A-5 for comparison. To realize these operating parameters in the existing test setup, a 0.25-Ω, 100-nH impedance capable of operating at 120 kV, 250 kA, and 27 kJ was designed and installed. A copper right-circular cylinder, 23-cm diam by 31-cm high, with a 2.5-cm-diam by 31-cm-long copper rod suspended along its axis, was used as both container and electrode for a solution of copper sulfate. Changing the concentration of $CuSo_4$ permitted adjustment of the series resistance; the inductance was not (easily) adjustable and was measured to be 120 nH. The load was arbitrarily adjusted for 18% current reversal, resulting in an I_{peak} of 225 kA, 0.63 C, and T = 7.9 μs. Actual gas-pulser values are 250 kA, 1 C, and T = 7.4μs.

E. Jitter Test

The switch was tested for jitter at different operating voltages and pressures with the $CuSO_4$ load installed. The test results are shown in Figs. A-6 through A-10. The trigger voltage amplitude and waveform was held constant for all jitter measurements. A 500-Ω $CuSO_4$ resistor was inserted in series with the trigger electrode to simulate the gas-pulser circuit values. The total spread is about 10 ns, implying a standard deviation on the order of 5 ns. The effect of trigger amplitude on jitter is shown in Figs. A-11 and A-12. A Hewlett-Packard Co. 5370-A time interval counter corroborated the oscilloscope data.

III. DETAILS OF THE SWITCH DEVELOPMENT

A. The Insulating Housing

The first failure experienced during the preliminary worst case fault testing of the purchased spark gaps was the explosive shattering of the 1.27-cm-thick insulating housing, fabricated from acrylic, used in two of the submitted designs. The third design used 0.635-cm-thick cast polyurethane (unfilled), which was even weaker in mechanical impact strength. The acrylic housings would operate a few hundred shots before shattering. These were replaced with 1.52-cm-thick cast nylon machined from tubular bar stock. Cast nylon has higher tensile, impact, and flexural strengths, and better heat resistance properties than acrylic (see Table A-I). No further problems with housing failures were experienced during extensive testing.

B. Through-Rods

The 1.27-cm-diam threaded nylon through-rods holding each unit together under compression had a low modulus of elasticity and would stretch significantly under impulse loading, resulting in short-duration air surges leaking past the O-ring seals. Some testing had been done on a relatively new product, basically a polyester resin and a reinforcing fiber glass core, "pultruded" into a rod and threaded. These rods are manufactured by Permali, Inc. under the trade name Superstud, and exhibit excellent high-voltage performance in mineral-base transformer oil with the advantage of very high tensile strength, modulus, and no detectable contamination by the transformer oil or moisture. The nylon rods were replaced with six 3/4-10, or eight 5/8-11 Superstud rods, depending on the design being tested. It was necessary to torque the nuts on each set in a cross-alternative pattern to 25 or 20 ft-lbs, respectively, to reduce the pulse air leaks to a minimum. The nuts used were either standard steel or glass/epoxy

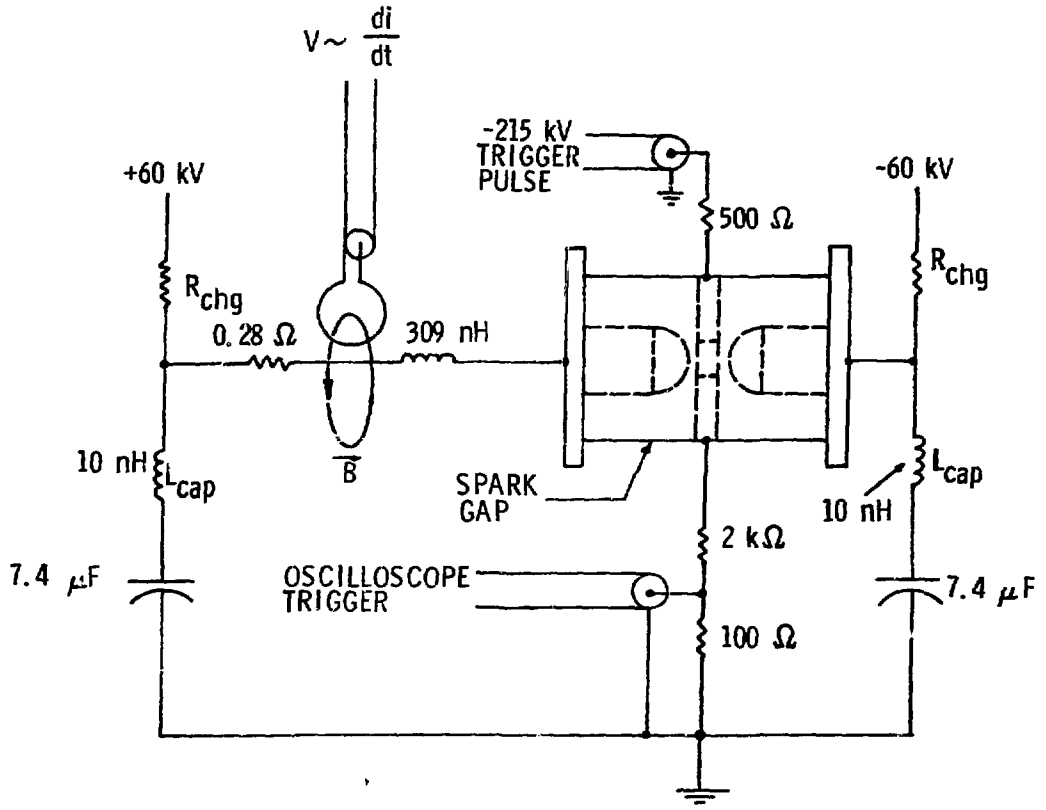

Fig. A-4.
Test circuit for jitter measurements.

composition. Glass nuts are recommended because they do not cut the threads on the rods as do the steel nuts if overtightened.

C. O-Ring Groove Size

The O-ring grooves had to be redesigned from the standard size for a 15.88-cm by 0.353-cm neoprene O-ring. We found that pulse air leaks occurred even when the through-rods were tightened to maximum compression. Under the high compressive forces of the through-rods, the O-ring compression was limited by the groove cross-sectional dimensions. No significant stretching of the through-rods was possible because of the very high modulus of elasticity; the pulse air leaks were a result of O-ring "blow-by," which was eliminated

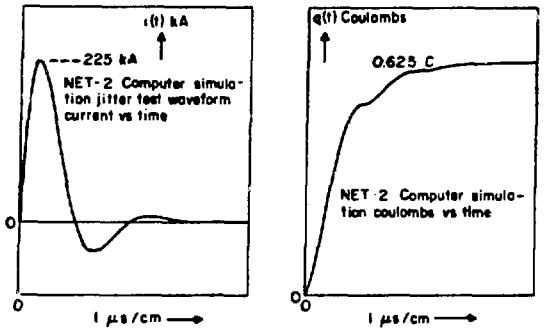

I (peak)	= 225 kA
V holdoff	= 120 kV
q per shot	= 0.625 C
Energy switched	= 27 kJ
f ring-down	= 127 kHz
Repetition rate	= 1 shot/min

See Fig. A-4 for test circuit and oscilloscope waveform.

Fig. A-5.
Jitter test circuit parameters.

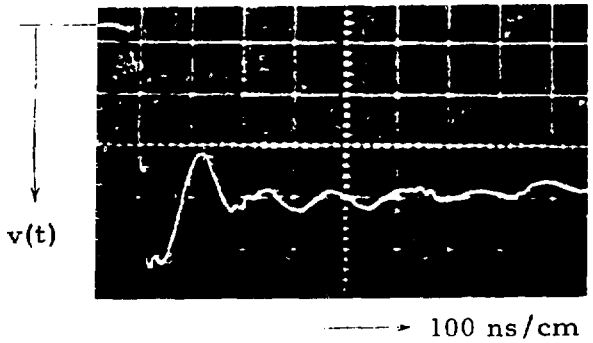

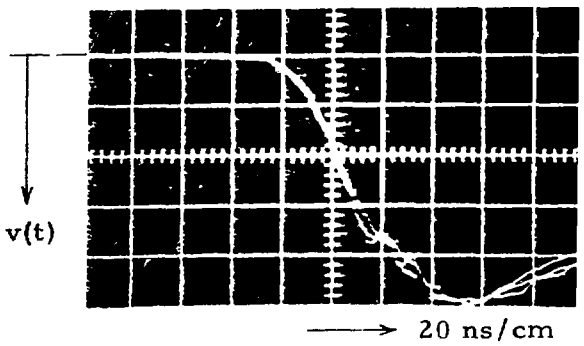

Fig. A-6.
Trigger generator waveform for jitter mesurements.

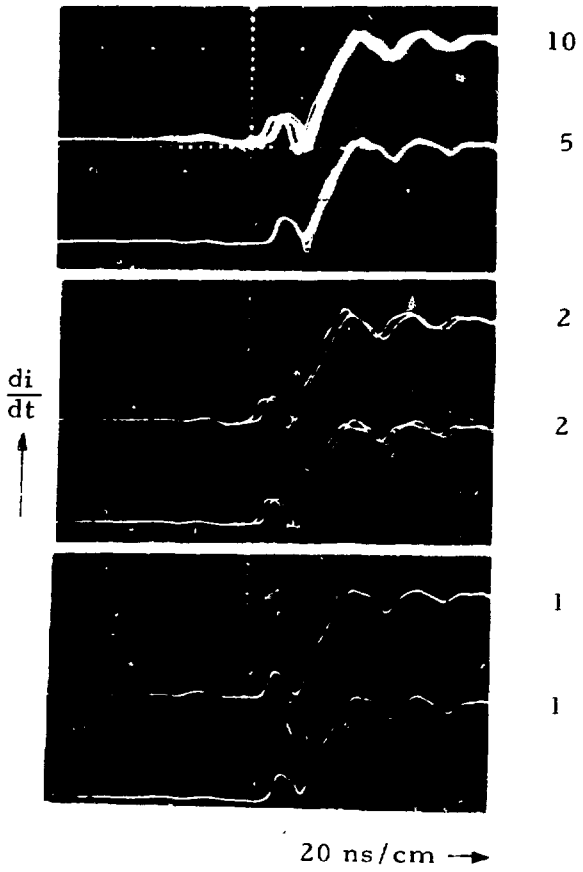

Fig. A-7.
Waveforms from spark-gap jitter test for 120 kV 60 psig-air M = 2.

by increasing the O-ring compression. A square bottom groove 0.229-cm deep by 0.445-cm wide (having a cross-sectional area equal to that of the O-ring) resulted in a reliable seal against the internal pressure impulse. Viton O-rings are recommended for their oil resistance. It is advantageous to increase the groove major diameter slightly beyond that of the O-ring, so that when the O-ring is stretched into place, it holds itself securely in the groove, facilitating assembly.

D. The Trigger Rail

One spark-gap design, with a rail or bar structure for a trigger electrode, was tested briefly. The mechanical integrity of the housing and rods suffered the same structural deficiencies as the other two designs; however,

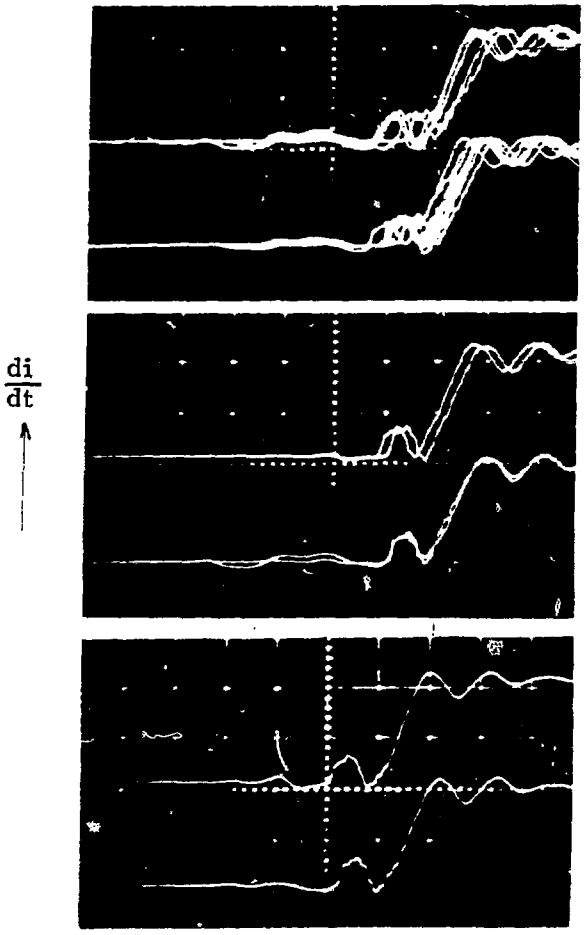

Fig. A-8.
Waveforms from spark-gap jitter test for 80 kV 34 psig-air M = 2.

the trigger rail presented a different problem. The rail was fabricated from a copper-tungsten composite and brass, brazed together to form a rail 12.7-cm long by 0.635-cm thick by 1.9-cm wide, with a full radius on both edges. It offered very good triggering and self-breakdown characteristics, requiring less trigger voltage to initiate the switch and exhibiting less spread in the static self-breakdown data. However, the rail eroded quite rapidly at its edges near the center of the air gap. After 300 worst case shots, both edges had eroded approximately 0.13 cm, and the rail's triggering effectiveness was impaired. It was replaced by a similar structure (6.35 cm in length, hence mechanically stronger) of commercially pure molybdenum, but the rail shattered after a few shots. Molybdenum was evaluated to select among properties: it is characterized by good high-temperature strength, brittleness at room temperature, and poor thermal and electrical conductivity (as compared to copper, brass, and copper-tungsten composites). Another rail identical to the original was fabricated from zirconium-copper (1% Zr: 99% Cu). No difficulties were experienced except that this rail eroded very rapidly at its edges. A more detailed discussion of the properties of electrode materials is presented in Sec. IV of this Appendix.

Experimentation with the trigger-rail configuration was abandoned because of

- the inherent mechanical stress problems caused by geometry,
- the higher fabrication costs (compared to disks),
- additional K25 copper-tungsten was not deliverable to meet the schedule, and

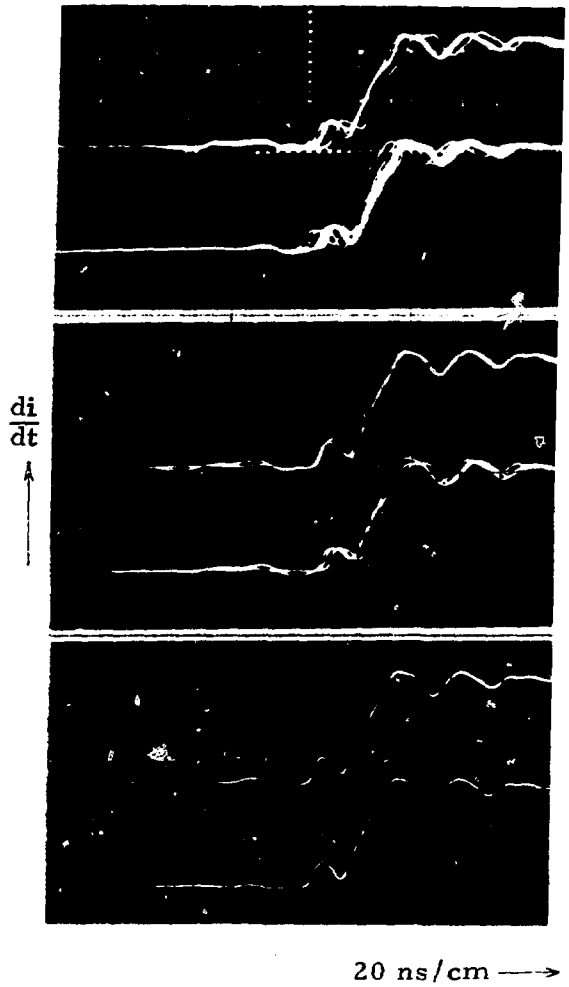

Fig. A-9.
Waveforms from spark-gap jitter test for 120 kV 50 psig-air M = 1.75.

- past experience has shown the trigger disk configuration to be operationally acceptable for this application.

The performance of the rail configuration in the static self-breakdown tests was encouraging. K25 composite should be tried for rail material, and jitter tests should be performed if the K25 rail proves to be adequate in mechanical strength and erosion resistance.

E. Plasma Splatter Shield

We tried one spark-gap design that included an aluminum cylindrical splatter shield, or shroud, concentric with the axis of the main electrodes in an attempt to prevent surface contamination of the insulating housings by the effects of the arc. The shroud was fabricated from 0.13-cm-thick aluminum and consisted of two halves fastened to each side of the midplane trigger electrode holder with eight 6-32 steel screws. The pressure shock generated by the rapid initiation of the plasma caused the shroud to deform (bulge outward) and the steel screws to loosen and fall out. The shroud was too close to the main electrodes (1.9 cm) and interfered with the self-breakdown and triggering characteristics, causing a large spread in the self-breakdown data and lowering the average breakdown voltage for a given gas pressure. The added capacitance between the trigger electrode and the main electrodes increased the loading on the trigger generator, resulting in an increased triggering difficulty, which was overcome by increasing the magnitude of the trigger voltage by approximately 25%. The shroud would intermittently behave as an electrode; the arc from the main electrode impinging on its inner surface caused

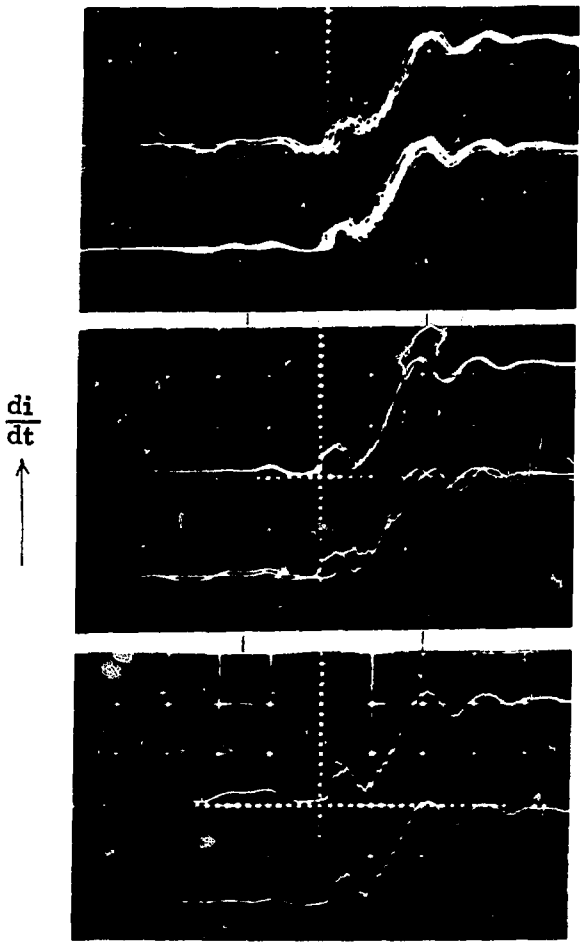

Fig. A-10.
Waveforms from spark-gap jitter test for 80 kV 27.6 psig-air M = 1.75.

current to flow along the shroud, through the midplane electrode holder, and onto the opposite shroud half. The electrical contact between the aluminum shroud halves and the aluminum trigger disk holder was only marginal, and rapid contact erosion occurred at these junctures. The shroud was eventually removed. Subsequent testing has proven that shielding the plasma to prevent insulator surface contamination is not necessary, at least when the insulator material is cast nylon and the gas is air.

F. SF_6 Dielectric Gas

Some experimental efforts were made to use SF_6 as a gas instead of purified dry air because the electrode spacing can be smaller and the pressure can be lower. Smaller electrode spacing results in less scatter in the static self-breakdown data for the same electrode diameter.[2] However, the use of SF_6 has several disadvantages. The cost of the gas is many times that of dry air. SF_6 has a large absorption coefficient for 10.6 μm radiation, making any gas leaks to the atmosphere in the vicinity of a CO_2 laser unacceptable. The generation of active fluorines by the plasma accelerates electrochemical corrosion of metals, especially aluminum. We experienced several problems when aluminum parts interior to the gap deteriorated into a white powder where large currents were flowing through a poor contact surface. (The powder was chemically analyzed and found to be aluminum fluoride.) Because the disadvantages outweigh the advantages, experimentation with SF_6 as a dielectric gas was discontinued.

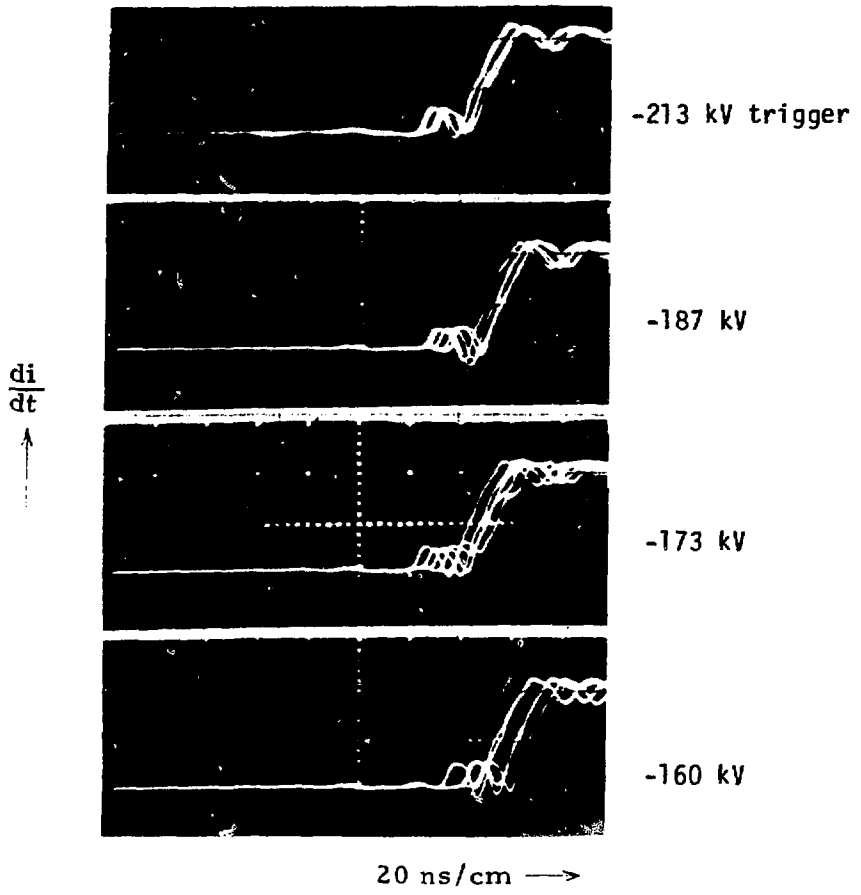

Fig. A-11.
Waveforms of jitter vs trigger amplitude for 120 kV 60 psig-air M = 2.

G. End Plates

We determined that type 6061-T6 aluminum was adequate for the end plates of the spark gap. The plates are far enough removed from high field regions and plasma to prevent arc impingement or surface heating, which accelerates electrochemical corrosion. However, certain precautions should be taken to avoid problems. Castings can be undesirable because of microscopic voids and surface irregularities which make it difficult to obtain good electrical contact between surfaces. Machining of a poor quality aluminum casting to improve surface quality may not be sufficient. The plates should be machined from bar or plate stock which has been heat-treated (T6) and worked. The finished plate has to be thick enough to prevent temporary deformation during impulse loading; otherwise, the mechanical integrity of the O-ring seals and the electrode hold-down rods is suspect. Axial concentricity of the main electrodes is preserved by machining a flat-bottomed circular groove in the end plates as a seat for the electrode standoff. This groove also assures that the electrode hold-down bolt is perpendicular to the end plate when tightened. Surface finish on the groove seat should be quite smooth to assure adequate electrical contact with the electrode stand-off. The recessed flat for the nylon insulator ends has a shoulder that mates with the outside diameter surface of the nylon and restrains the insulator, enhancing its impact strength during impulse loading. This feature also is present on the trigger disk holder at the opposite end of the insulator. The tolerance between the nylon and the restraining shoulder is close; therefore,

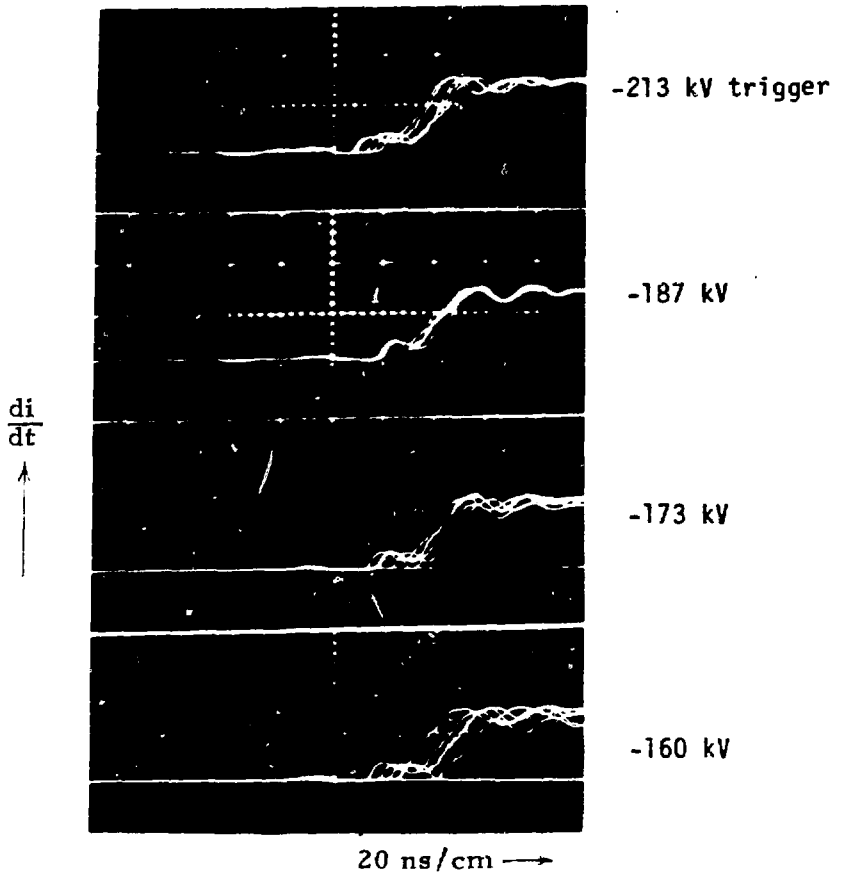

Fig. A-12.
Waveforms of jitter vs trigger amplitude for 80 kV 34 psig-air M = 2.

these parts should be fabricated on a machine-to-fit basis. The parts will not be completely interchangeable, but this method will be most cost effective.

H. Trigger Disk Holder

Arc impingement on the aluminum trigger disk holder and the resulting current flow between the trigger electrode material and the aluminum caused corrosion problems as the aluminum shroud did. A brass holder was designed with careful attention to the radii mating into the electrode surfaces to prevent arc impingement on the holder. The trigger disk was fastened to the holder with eight 4-40 steel screws with lockwashers, and the protruding screw ends were peened and machined flush with the holder surface. The brass holder worked quite well, showing very little deterioration from occasional arcs. The screws, however, loosened, which allowed the trigger disk to vibrate slightly in the holder. Good thermal contact between the trigger disk and holder is necessary to prevent overheating the disk, which aggravates erosion, warping, and cracking. A tapered steel snap ring and tapered groove were used to seat the disk firmly in the holder. The tapered snap ring groove had to be redesigned from the manufacturer's specifications so that the ring would hold tension on the disk; otherwise, the ring bottomed on the groove, and no axial force was exerted by the tapered mating surfaces.

I. Dezincification of Brass

A bluish-colored powder, present in modest quantities after many test shots, suggested a possible problem with dezincification of the brass, which is, to a small degree, incipient at room temperature. Because the spark gap

TABLE A-I
PHYSICAL PROPERTIES OF ACRYLIC VS CAST NYLON

Physical Properties	Acrylic	Cast Nylon
Tensile Strength (10^3 psi)	8 – 11	11 – 14
Impact Strength - Izod (ft-lbs/in.)	0.4 – 0.5	1.2 – 2.5
Flexural Strength (10^3 psi)	12 – 17	16.5 – 17.5
Modulus of Elasticity (10^5 psi)	3.5 – 5	2.6 – 4
Continuous Heat Resistance (°F)	140 – 200	350
Heat Distortion Temperature (°F)	150 – 210	410 – 420
H_2O Absorption (%/25 h)	0.3 – 0.4	0.06
Elongation (% at yield)	2 – 7	10 – 60

was mounted with its longitudinal axis horizontal, the powder (probably zinc oxide) accumulated by gravity on the upper surfaces of the standoffs and the bottom interior surfaces of the nylon. To avoid any future problems with this powder or the brass, a readily available aluminum bronze alloy (No. 618) was used as the fabrication material for the standoffs and the trigger disk electrode holder. Subsequent testing of the spark gap at worst case fault and normal power levels has revealed no evidence of this powder.

J. Electrode Spacing for Air

The air-gap spacing between the main hemispherical electrodes was determined by several factors.

- The spacing must be small enough so that a positive gas pressure is required at 40 kV and M = 1.7. (During purge, the pressure must be increased to obtain a flow rate of 3 scfm or better.)
- The spacing must be large enough so that the gas pressure at 120 kV and M = 2 is within a reasonable limit as constrained by the strength of the spark-gap housing and through-rods vs the peak pressure generated when the gap is fired.
- The ratio of gap spacing to electrode hemisphere diameter must be such (≤ 0.5) that there is an acceptably small spread in the self-breakdown data for a constant gas pressure.[2]
- The diameter of the hemispherical electrodes is constrained to a maximum of 5 cm because of electrode-to-insulating-housing spacing considerations.[3]

Trial and error experiments with electrode gap spacing and self-breakdown voltage produced an optimum air gap of 2.79 cm. With this spacing, the air pressure

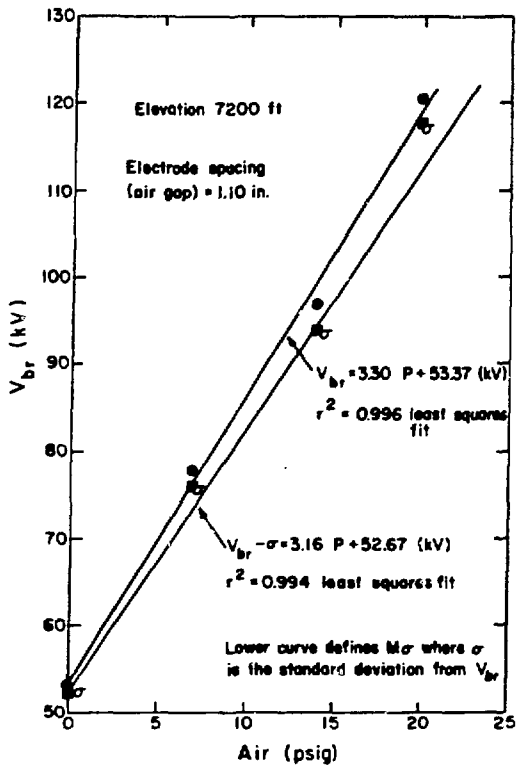

Fig. A-13.
Spark-gap self-breakdown voltage vs dielectric gas pressure (air).

required for an M = 2 at 120 kV is 60 psig; the pressure for an M = 1.7 at 40 kV is 5 psig, with $\sigma/V_{br} \cong 0.03$.

A plot of self-breakdown voltage vs air pressure is shown in Fig. A-13. Each point on the curve represents 30 slow-charge, self-breakdown trials at a constant gas pressure. Plotting $\bar{V}_{br}$ vs P results in a straight line from which larger values of V and P are projected for a constant M value. The standard deviation at each (V, P) value is plotted as $\bar{V}_{br} - \sigma$ vs P. This straight line defines m_σ and larger values of V or P are projected from this line. The m_σ plot is more meaningful and conservative than V_{br} vs P; thus, the switch is operated and was tested at $m_\sigma = 2$ (Fig. A-13).

K. Considerations for Purging of Breakdown Products

The gas-line fittings should not be sealed with Teflon pipe tape because injection of Teflon fragments into the spark gap could cause undesirable prefires; rather, conservative use of a pipe thread sealant such as Rectorseal is recommended. The purging mechanisms are important because they affect the performance of the spark gap. One obvious purpose of purging is the elimination of gaseous products, such as ozone, and the replenishment of the gas. To avoid low flow "channeling," adequate turbulence is necessary and most easily accomplished by high flow rates. Another goal is elimination of particulates. Again, it is necessary to use high flow rates to create turbulence and to overcome particulate surface adhesion and gravity effects. An oversupply of oxygen impinging on hot electrode surfaces can be detrimental to electrode life, increasing erosion or oxidation of the electrode; therefore, purge flow rate should be adjusted to some maximum that does not greatly accelerate electrode erosion. Alternatively, the delay time between a shot and initiation of purge may be adjusted to allow the electrode surfaces to cool. Ideally, the optimum delay time is a function of spark-gap conduction parameters (peak current, voltage, and charge) that determine the heating of the electrode surfaces.

IV. ELECTRODE MATERIALS

The contractor-furnished electrodes were made of one of two materials: tungsten or copper filled with tungsten powder. Neither worked at our current of 400 kA, but the electrodes functioned well at the usual current of 200 kA. We decided to try three materials that differed not only from each other, but also from the original two candidates (see Table A-II). Molybdenum failed quickly; it also demonstrated that reducing ductile to brittle transition temperature from 675°C (for tungsten) to 68°C (for molybdenum) had no noticeable effect. We felt it probably confirmed a need for better electrical conductivity.

Zirconium copper also was tested. This copper alloy is one of the best for both strength and higher-than-usual operating temperatures. All coppers are well-known for their rapid loss of strength with increasing temperature. The electrodes failed after only a few shots. A rather cursory visual examination seemed to indicate the problem was localized melting.

The third material tried was a tungsten matrix filled with copper. Two sources of such a composite were located: Teledyne Wah Chang in Albany, Oregon, and Metalwerke Plansee in Reutte, Austria. Teledyne produces copper-filled tungsten at approximately 11 wt%

TABLE A-II
METALS INVESTIGATED

Metal	Electrical Conductivity	High Temp Strength	Room Temp Impact Strength	~ 900°C Impact Strength
Molybdenum	Fair	Excellent	Very Poor	Excellent
Zirconium Copper	Excellent	Poor	Good	Poor
Tungsten-filled copper matrix	Good	Poor	Poor	Poor
Copper-filled tungsten matrix	Good	Excellent	Poor	Excellent

copper in volume as an ablation shield in rocketry; therefore they do not offer other compositions of the material. Plansee, on the other hand, offered the material in a complete range of compositions. They have developed a unique reduction process, from WO_3 rather than WO_2, which yields powders tenfold the usual diameter, and hence well suited for a more open mesh and higher percentage of copper. We tested a composition "K-25" (25 wt% copper), which worked very well. The tungsten powder was sintered at approximately 2200°C and then infiltrated with liquid copper. No subsequent working, that is, by forging, rolling, swaging, etc., was done. Plansee has continued to experiment with the composite and reports that "K-33" (33 wt% copper) performs even better.

The total success of this composite seems to indicate the following conclusions.

- Good electrical conductivity is required.
- High termperature strength is vital.
- Room temperature impact strength is not required.

A tungsten matrix was evaluated because work done by Metalwerke Plansee, although directed at a totally different application, provided us with valuable information about tungsten. A molybdenium matrix couid prove just as satisfactory at half the cost.

REFERENCES

1. G. N. Glasoe and J. V. Lebacqz, *Pulse Generators*, (Dover Publications, Inc., New York, 1965), p. 280.

2. L. L. Alston, *High-Voltage Technology*, (Oxford University Press, London, 1968), p. 15.

3. J. D. Cobine, *Gaseous Conductors*, (Dover Publications, Inc., New York, 1958), p. 171.

APPENDIX B
CAPACITOR TESTING

The capacitors used in the Marx are 2.8 μF rated at 60 kV. Models of this capacitor manufactured by Aerovox Industries and by Maxwell Laboratories, Inc. were qualified for use under low-reversal conditions in the Scyllac program. Their behavior under short-circuit, high-reversal conditions had not been tested.

In the event that the Marx output is short-circuited, the capacitor will ring at 130 kA with reversal near 90% (limited only by capacitor internal resistance and switch resistance). We were worried primarily that the high current would damage the swaging between the capacitor pads and the current collector plate and that the high voltage reversal would damage the dielectric.

The test arrangement used two oppositely charged capacitors facing each other with a spark gap connecting the high-voltage terminals and the cases of the capacitors connected. Triggering the switch shorted the capacitors through each other and produced a high-reversal, ringing discharge. The total inductance of the test circuit was 300 nH; measured reversal was 85%, producing a peak current of 240 kA for a 60-kV charge. Because the greatest interest was in the behavior of the swaging, the charge voltage was reduced to 50 kV to extend the dielectric life, producing 200 kA peak current. Two capacitors were run, one for 4070 shots, the other for 5000 shots, and then dissected. Damage to the capacitors was negligible. We concluded that the capacitors will be able to handle the conditions in the Antares gas pulser with no problems.

APPENDIX C
RESISTOR DEVELOPMENT

Most Marx generators have used liquid resistors for stage charging isolation and trigger coupling. Liquid resistors have the advantage of large energy-handling capability, physical flexibility, and easy resistance-value adjustment. We felt that liquid resistors would not provide the reliability required in this large system because of their propensity to leak.

Two types of solid resistors were tested: wire-wound and Carborundum-type AS. The test consisted of discharging a 170-μF capacitor at charge voltage up to 11 kV (10 kJ) into the resistor. Evidence of failure would be visible physical damage to the resistor or significant change in value. The resistors were first soaked in transformer oil. The wire-wound resistors were Dale 225 W, 100 Ω. At 1/2 kJ their coating melted.

The Carborundum resistors were type 889AS (12 in. long, 1 in. diam). Uncoated, these are rated by the manufacturer at 35 kJ in air. The manufacturer recommends coating the resistors with epoxy if they are to be used under oil; otherwise, they will absorb oil and increase in value. We also found that oil-soaked resistors can handle much less energy, failing at 3 kJ by chipping. Apparently this is due to rapid heating and expansion of the oil within the resistor body. The standard epoxy coating from Carborundum did not fare any better because pinholes in the coating allowed oil to leak into the resistor body. Carborundum eventually developed a laminar coating that enabled the resistors to run up to 10 kJ, the limit of our test facility, without failure. This provided an adequate safety margin for use in the Marx generator.